ACS APPLIED MATERIALS & INTERFACES

www.acsami.org Research Article

Stretchable Gas Barrier Films Using Liquid Metal toward a Highly Deformable Battery

Nyamjargal Ochirkhuyag, Yuuki Nishitai, Satoru Mizuguchi, Yuji Isano, Sijie Ni, Koki Murakami, Masaki Shimamura, Hiroki Iida, Kazuhide Ueno, and Hiroki Ota*

Cite This: https://doi.org/10.1021/acsami.2c13023 Read Online

ACCESS | Metrics & More | Article Recommendations | Supporting Information

ABSTRACT: Highly deformable batteries that are flexible and stretchable are important for the next-generation wearable devices. Several studies have focused on the stable operation and life span of batteries. On the other hand, there has been less focus on the packaging of highly deformable batteries. In wearable devices, solid-state or pouch lithium-ion batteries (LIBs) packaged in aluminum (Al)-laminated films, which protect against moisture and gas permeation, are used. Stretchable elastomer materials are used as the packaging films of highly deformable batteries; however, they are extremely permeable to gas and moisture. Therefore, a packaging film that provides high deformability along with gas and moisture barrier functionalities is required for the stable operation of highly deformable batteries used in ambient conditions. In this study, a stretchable packaging film with high gas barrier functionality is developed successfully by coating a thin layer of liquid metal onto a gold (Au)-deposited thermoplastic polyurethane film using the layer-by-layer method. The film exhibits excellent oxygen gas impermeability under mechanical strain and extremely low moisture permeability. It shows high impermeability along with high mechanical robustness. Using the proposed stretchable gas barrier film, a highly deformable LIB is assembled, which offers reliable operation in air. The operation of the highly deformable battery is analyzed by powering LEDs under mechanical deformations in ambient conditions. The proposed stretchable packaging film can potentially be used for the development of packaging films in advanced wearable electronic devices.

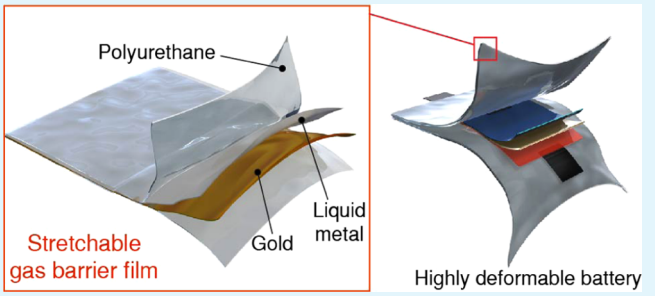

KEYWORDS: *stretchable, impermeable, liquid metal, thermoplastic polyurethane, highly deformable battery, layer by layer*

1. INTRODUCTION

Wearable electronics applications are being extensively applied in various fields, including medical devices, sensors, soft robotics, and drug delivery.[1−3] These devices can be either battery-free or battery-powered; however, integrating them with batteries is necessary for ensuring a stable power supply and reliable operation.[4,5] To realize a stable power supply for wearable electronics applications, high-performance power supplies must be flexible and stretchable while maintaining excellent electrochemical performance. Such power supplies can be categorized into supercapacitors, which offer high power density and long-term cyclability, and batteries, which offer high energy density, high working voltage, and long-term stability. Batteries are more suitable for wearable devices than supercapacitors in terms of energy density.[1,6] Studies have focused on developing batteries that are flexible and stretchable[1] while offering advantages such as long life, electrochemical stability under deformation, higher capacities, and convenient outer designs or shapes. Therefore, they are considered a promising power source for next-generation wearable electronics.

Although the packaging for highly deformable batteries is an important consideration, limited literature is available. One possible approach for incorporating highly deformable batteries in wearable electronics is by replacing stiff materials with soft and flexible materials while also ensuring stable performance under deformation. To guarantee stable performance, the deformable packaging should prevent leakage and evaporation of electrolytes and protect the battery against moisture and gas permeations. Thus, it should provide long-term stable operation in ambient conditions.[7,8]

The packaging material should be highly stretchable, deformable, and impermeable to moisture and air to avoid undesirable side effects in the batteries. Additionally, it should enable stable battery operation under deformations such as bending, twisting, folding, and stretching. Stretchable elas-

Received: July 20, 2022
Accepted: September 20, 2022

tomers, such as polydimethylsiloxane (PDMS) and Ecoflex, are commonly used as packaging materials for deformable batteries.[1,9,10] Moisture and gas permeabilities of these elastomers are significantly higher than that of an aluminum (Al)-laminated film used in commercialized lithium-ion pouch cells, which makes them unsuitable for packaging lithium-ion batteries (LIBs). Therefore, stretchable material with low gas permeability is needed. In this study, a stretchable packaging film with high gas barrier behavior for highly deformable batteries is fabricated. The stretchable packaging film (gas barrier film (GBF)) has a high gas impermeability and is slightly permeable to a low amount of moisture. Thermoplastic polyurethane (TPU) and liquid metal (LM) are the two main layers of the GBF. An LM layer is sandwiched between two layers of TPU. The LM employed consists of gallium (Ga) and tin (Sn) and is widely used in flexible or wearable electronics because of its high electrical conductivity, stretchability, and property of being in a liquid state at room temperature. The stretchable LM layer sandwiched between two TPU layers satisfies both barrier functionality and elasticity, thereby maintaining the stability of the components inside an LIB placed in air. The highly deformable LIB assembled using the GBF exhibits an excellent performance even under mechanical deformations in ambient conditions. The highly deformable battery can be deformed by a 50% stretching, a 90° bending, and an approximately 25° twisting. The electrochemical measurement of the highly deformable battery is carried out at the original state and during a stretched state with a stretching strain of 50%. Although its capacity drops by 50% under the stretching state, the good performance of the battery demonstrates its capability of working under mechanical deformations. Moreover, the highly deformable battery can maintain its stable operation in air for longer than 14 h.

2. EXPERIMENTAL SECTION

2.1. Materials. *N*-Methyl-2-pyrrolidone (NMP) from Kanto Chemical Co., Inc., 1-butanol and hexane from Fujifilm Wako Pure Chemical Corporation, and polystyrene-*block*-polybutadiene-*block*-polystyrene (SBS) from Sigma-Aldrich were used. Ga and Sn elements in the LM were purchased from Zairyo-ya.com and Nilaco Corporation, respectively. TPU pellets (Elastollan 1180A) from BASF Japan Ltd. were used. The key materials of the GBF are TPU and LM, which enhance the impermeabilities.

2.2. Fabrication of the Stretchable Gas Barrier Film (GBF). First, a base for the GBF was prepared using the TPU film. The TPU elastomer pellets were dissolved in the NMP organic solvent, in a weight ratio of 1.5:12, and stirred overnight. Thereafter, it was drop-casted onto a glass substrate and heated at 80 °C for 12 h on a hot plate. It was then placed in a vacuum oven at the same temperature for 2 h. Second, a thin Au layer was deposited on the TPU film using physical vapor deposition (PVD). The thickness of the Au layer was 100 nm, which was sufficient to coat the LM on it. Third, a thin layer of the LM was coated uniformly onto the Au-deposited TPU film by a printing method. Ga and Sn were melted and mixed in a vial at 250 °C for 30 min. Three thin layers of the LM were coated, at an interval of 1 h, with a total thickness of approximately 10−15 μm. Lastly, the TPU solution was again drop-casted onto the LM-coated TPU film to seal the edges and form the final layer of the GBF, whose thickness varied between approximately 210 and 340 μm. From a cost perspective, the appreciable thickness of LM for realizing the impermeability can be determined as approximately 11.23 μm. The gas and moisture permeabilities can be sufficiently prevented by adopting LM thicknesses of more than 4.5 and 11.23 μm, respectively. Hence, the GBF was fabricated using a layer-by-layer method, and the fabrication process is illustrated in Figure S1. The Au layer deposited on the TPU film acted as an adhesion layer for easy coating of the LM, owing to its metallic bonding. LM can be deposited onto the TPU film directly, but because of its bad wettability, the process becomes challenging. Figure S2 compares the TPU films with and without the Au layer. Figure S3 shows a contact angle of 130 and 78° between the TPU-LM and Au-LM layers, respectively.

2.3. Tensile Strength Measurement. The measurements were conducted using Shimadzu EZ-LX tensile strength equipment. A power scale of 10 N and a speed of 0.5 cm/min were set as the measurement conditions. Samples of the TPU, TPU/Au, and TPU/Au/LM films were prepared and cut into shapes of dumbbells. The thickness of the samples varied between 199 and 274 μm.

2.4. Repeatability Measurement. The measurement was conducted using HSC-103 three-axis motion controllers with a single-axis stage from OptoSigma, Japan, and an Imada force measurement gauge. The GBF was secured on the single-axis stage, and the Imada force measurement gauge was positioned in the targeted position of the single-axis stage for measurement. On the HSC-103 motion controller, the measurement conditions were set using a 50% stretching with 200 stretch−release cycles.

2.5. SEM−EDX Analysis. SEM−EDX images were observed using a Hitachi SU8010 scanning electron microscopy and a Bruker Quantax Esprit 1.9 X-ray spectroscopy. The accelerating voltage for the analysis was set to 10 kV, in accordance with the X-ray characteristics of Ga and Sn, which are higher compared to those of Au and C. Image scale of the analysis for both surface and cross section was 100 μm. Peaks of all elements were observed at 10 kV. A cross section of the GBF is presented in Figure S4A.

2.6. Gas Permeation Measurement. The gas permeation values were measured using the GTR-10XFYU gas permeation measurement system from Yanaco Analytical Systems Inc., where oxygen and helium were used as test and carrier gases, respectively. The principle of measurement is shown in Figure S5. The GBF was placed in a test cell chamber, and the gases, at the same pressure of 250 kPa, were introduced. The oven and detector were set at 80 and 150 °C, respectively, on the gas chromatograph. The flow rates of the test and carrier gases were set to 30 and 50 cc/min, respectively, and the pressure on the gas permeation meter was set to 250 kPa. The measurement was performed at 30 °C with an average flow rate of 44 mL/min. Measurements were conducted with these conditions set on the equipment.

2.7. Moisture Measurement. Moisture permeations were measured in an ESPEC SH-241 environmental chamber with conditions set to 25 °C and 30% humidity. Five samples of the Al-laminated film, GBF, TPU, PDMS, and Ecoflex-0030 films were prepared. Thereafter, small vials were filled with 10 mL of water, and the samples were secured on top of these small vials. The vials were weighed before being placed in the environmental chamber. Then, they were weighted every hour for 10 h. Furthermore, they were also weighted after 24 and 72 h.

2.8. Flexible Electrodes and Gel Electrolyte Preparation. Flexible or stretchable electrodes were prepared based on the SBS block copolymer porous membrane, which was discussed in a previous study.[11] Once the SBS porous membrane was prepared, they were cut to a size of 2 cm×1 cm. Thereafter, the flexible electrodes were fabricated by spray printing a slurry solution of active materials onto the SBS membranes. The slurry solutions constituted Li4Ti5O12 (LTO) and LiFePO4 (LFP) as the anode and cathode, respectively, super P as the conducting carbon, and poly(vinylidene-fluoride) (PVDF) as the binder. A weight ratio of 5:4:1 was maintained. Metal tabs were attached to the flexible electrodes by a conductive paste that was prepared by mixing super P, hexane, and Ecoflex-0030 in a weight ratio of 1:25:10. This was done to eliminate disconnections or weak connections between the electrodes and tabs.

The gel electrolyte was prepared using poly(vinylidene fluoride)−hexafluoropropylene (PVDF−HFP) as the polymer matrix and [Li(G4)] [TFSI] as the electrolyte.[12] First, the PVDF−HFP was dissolved in acetone and the liquid electrolyte was mixed with acetone in a weight ratio of 1:6 and 1:1, respectively, followed by a 15 min stir. Thereafter, the solutions were mixed together and stirred for 15−20

https://doi.org/10.1021/acsami.2c13023
ACS Appl. Mater. Interfaces XXXX, XXX, XXX−XXX

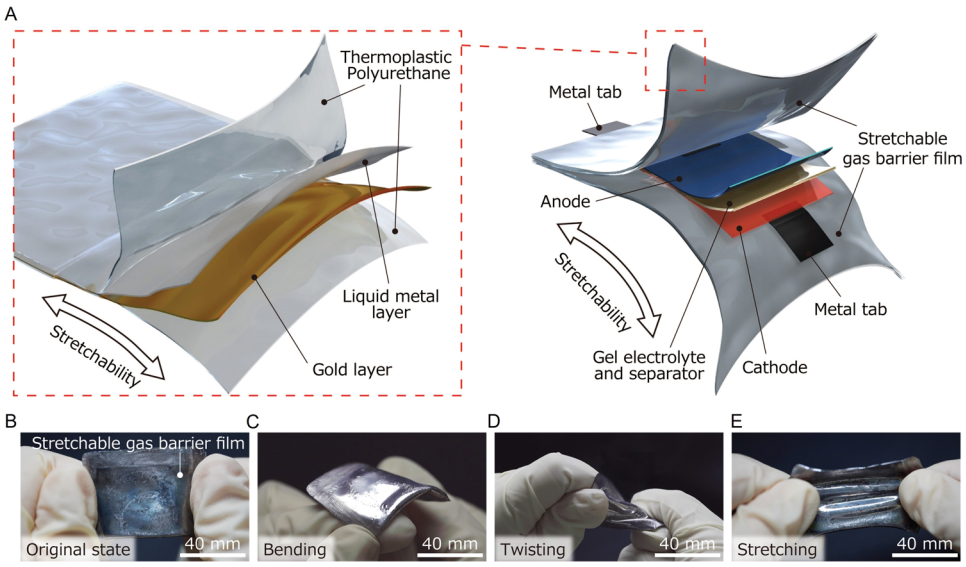

Figure 1. Stretchable GBF using liquid metal for a highly deformable battery. (A) Schematics of the stretchable GBF composed of LM, Au, and TPU layers and the highly deformable battery. Photographs of the highly deformable battery using the stretchable GBF. The highly deformable battery, which comprises of stretchable components, was deformed from (B) the original state by (C) bending, (D) twisting, and (E) stretching.

min. Subsequently, the mixture was poured into a Petri dish and stored in a dry box overnight to form the gel electrolyte.

2.9. Fabrication and Electrochemical Characteristics of a Highly Deformable Battery. Fabrication of the highly deformable battery was relatively easy. The metal tabs were attached to the electrodes by a conductive paste, and the gel electrolyte was placed between the two electrodes to act as an electrolyte and a separator. After placing the electrodes on the GBF, both sides were sealed. One hundred and fifty microliters of the liquid electrolyte was added to strengthen the wettability before vacuum sealing and completing the fabrication process. The fabrication process was carried out in a dry room. Charge−discharge measurements on the highly deformable battery were conducted using the Biologic-BT Lab electrochemical instrument, with a cutoff voltage of 1−2.5 V at 30 °C, and the cycling behavior of the highly deformable battery was evaluated. The stretchable electrodes were assembled as a coin cell, and its capacity was realized to be approximately 37 mAh/g, as shown in Figure S8A. Impedance measurement of the highly deformable battery was performed, as shown in Figure S9, and the resistances evaluated at the original and stretching states were approximately 300 and 650 Ω, respectively. These measurements were conducted before the charge−discharge measurement, in the frequency range of 10 mHz to 10 kHz, with an amplitude of 10 mV. The resistance increased by 2 times at a stretching state of 50% due to an increase in the ionic resistance of the porous and stretchable electrodes.

3. RESULTS AND DISCUSSION

Figure 1 shows the schematic of the stretchable gas barrier film (GBF), and photographs of the highly deformable battery developed using the GBF under various mechanical deformations, including bending, twisting, and stretching.

The stretchable GBF was fabricated using a layer-by-layer method, as seen in Figures 1A and S1. A thin layer of the LM was print-coated on the TPU substrate film and sealed by the TPU solution from the top. This method was beneficial, as it enabled various deformations unlike in Al-laminated films. The stretchability of the proposed GBF was better than that of the Al-laminated film. The highly deformable battery packaged in the proposed GBF was capable of working under various mechanical deformations. The thin Au layer deposited under the LM layer improved the wettability of the LM on the surface of the TPU film.[13] Figure S2A,B compares the two LM-coated TPU films, without and with the thin Au layer, respectively. As the LM formed a good connection by alloying with other metals, the smooth surface of the substrate improved the adhesion property or wettability of the LM.[13] Although the wettability of the LM could be improved by alloying, there were metals that could not be used for the LM deposition. According to the contact angles measured, as shown in Figure S3, Au and Cu had excellent wettability for easy LM deposition, in contrast to Ni and Sn, with which the LM could not be deposited properly. Similarly, the LM had a weak wettability on the TPU film. However, for experimentation, the LM was deposited onto the TPU film directly. A high gas impermeability was observed even with the pinhole coating, as shown in Figure S12. The LM prevents gas permeation due to its metallic nature. Metallic materials are known to show very low gas permeation properties that are attributable to strong metallic bonding. The strong interatomic interaction results in a high boiling point and surface tension of the metals. The LM has a surface tension of approximately 700 mN/m, which is similar to that of Al used in Al-laminated films and more than an order of magnitude higher than that of organic materials.[14,15] Therefore, the LM intrinsically shows low gas permeability like typical metallic solids. The surface oxide layer of the LM, which is a thin layer of Ga_2O_3 formed by exposure to air, also plays a role in gas impermeability of the proposed stretchable packaging film. A thin film of metal oxide itself has the potential to serve as a gas barrier layer similar to the atomic layer of deposited aluminum oxide (Al_2O_3) on polymer films.[16] This serves as an alternative to the metallized plastic packaging film. Similarly, the high gas barrier properties of the LM may be due to the thin layer of Ga_2O_3 on its surface. The GBF was tested by assembling a highly deformable battery, which was fabricated by wrapping the cathode and anode electrodes, and the gel electrolyte in the GBF. The fabrication process of the highly deformable battery was relatively easy compared to that of other deformable batteries, with external designs that may require a complicated fabrication process.

https://doi.org/10.1021/acsami.2c13023
ACS Appl. Mater. Interfaces XXXX, XXX, XXX−XXX

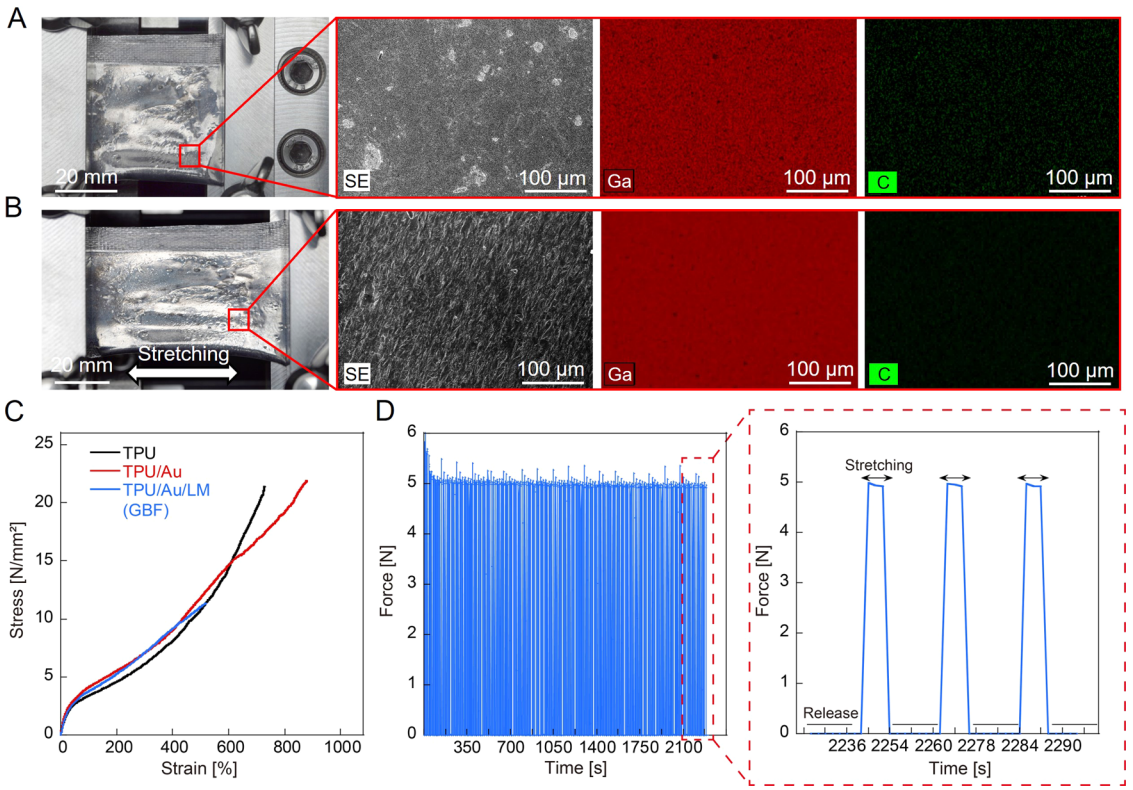

Figure 2. Mechanical properties of the stretchable gas barrier film. SEM−EDX images of the film surface (A) without stretching and (B) with stretching by 50%. (C) Stress−strain curve of TPU, TPU/Au, and GBF. (D) Repeatability tests of 200 cycles at a 50% strain.

3.1. Material Property. To characterize the behavior of the thin LM layer during stretching at a 50% tensile strain, the surface condition was analyzed using scanning electron microscopy (SEM) and energy-dispersive X-ray spectroscopy (EDX). The SEM−EDX analysis of the surface was performed to check for any disconnections formed during the stretching of the LM layer. As can be seen in Figure 2A,B, no cracks or breaks in the LM layer, which covered the entire surface of the TPU substrate film during stretching, were observed. This was confirmed by quantifying the material elements before (nonstretched state) and while stretching (stretched state). The detected quantity of Ga, one of the main components in the LM, was approximately more than 60% for both states, whereas the quantity of C, often detected on the TPU substrate film, was approximately 6% for both states. The quantity of C can be considered zero because it was negligible. Moreover, it is almost impossible not to detect C during the SEM−EDX because C can be detected even in materials that do not contain C. Although the thin Au layer on the TPU substrate film was cracked during stretching, as shown in Figure S4C,D, no impact was observed on the LM layer.[17,18] LM is known to be suitable for deformable or stretchable applications because of its ability to remain in the liquid state at room temperature. LM deposited on several elastomer materials, such as the TPU, PVDF−HFP, SEBS (styrene−ethylene−butylene−styrene thermoplastic polyurethane), PDMS, and Ecoflex films, was developed.[19−21] A maximum mechanical strain functionality of 1000% could be reached for the LM; however, the strain was dependent on the substrate materials.[19−21] The mechanical strains of the TPU, TPU film coated with a thin Au layer (TPU/Au), and TPU coated with thin layers of Au and LM (TPU/Au/LM) or the proposed stretchable GBF varied in the range of 500−900%, depending on the depositions. The stress−strain curves of the three films are compared in Figure 2C. It is observed that the strain of the GBF was reduced approximately by 42%, while maintaining the same stress, when compared to that of the TPU and TPU/Au films with a thickness of approximately 220 μm. The stiffness effect of the LM inclusions may have lowered the strain.[22] However, no cracks on the TPU, TPU/Au, and GBF were observed during the tensile strength measurement. Thus, the TPU film is considered to have a higher robustness when compared to the PDMS and Ecoflex-0030 films, which are more commonly used in stretchable or flexible film fabrication. Tensile strength measurement was conducted on the Au- and LM-coated PDMS and Ecoflex-0030. PDMS coated with thin layers of Au and LM (PDMS/Au/LM) was stretched to a maximum strain of 141% with Young's modulus of 24 kPa, whereas Ecoflex-0030 coated with thin layers of Au and LM (Ecoflex-0030/Au/LM) showed a maximum strain of 332% with Young's modulus of 880 Pa. Young's modulus of the GBF was calculated as 22 kPa at a maximum strain of 517%. Thus, the GBF had a higher strain with a low modulus compared to the Ecoflex-0030- and PDMS-based films.

To further investigate the robustness of the GBF, a repeatability test was conducted under a 50% strain with 200 stretch−release cycles, illustrated in Figure 2D. The force required for a 50% stretching was 5 N for each stretch−release cycle. Despite the 200 stretch−release cycles, no visible changes were observed in the GBF. Thus, the number of stretch−release cycles can exceed 200 because of the robustness and stretchability of the GBF.

TPU is an elastomer with high tensile strength, high elasticity, and low crystallinity. It consists of two segments, a

https://doi.org/10.1021/acsami.2c13023
ACS Appl. Mater. Interfaces XXXX, XXX, XXX−XXX

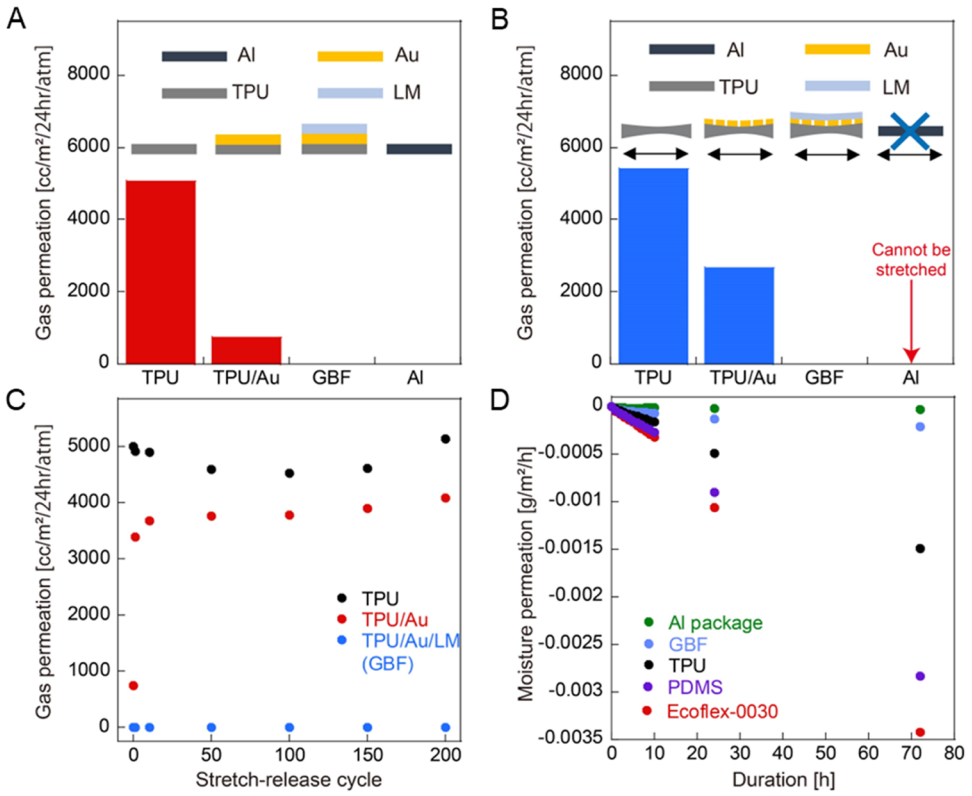

Figure 3. Gas and moisture permeabilities of the films. The gas transmission rate of the TPU, TPU/Au, GBF, and Al-laminated films during the (A) nonstretching state, (B) stretching state, and (C) after up to 200 stretch−release cycles. (D) Moisture permeation comparison among the stretchable GBF, TPU, PDMS, Ecoflex-0030, and Al-laminated films.

hard and a soft segment. The hard segments are interconnected throughout the soft segments, and they help maintain dimensional stability. Thus, the mechanical deformation of TPU can change depending on its composition as it is a high-quality material combining high elasticity with hardness.[23,24] As the hardness of TPU increases, its mechanical stress increases, but its mechanical strain decreases.[25] Soft segmented TPU can be stretched to more than 1000% strain at 5 MPa,[26] and waterborne PU can be stretched from approximately 800% to more than 1000% strain at 3 MPa.[27] However, hard segmented TPU can be stretched by less than 270% at 20 MPa[28] and glass-fiber-reinforced PU can only be stretched to 0.012 μm/m at 300 MPa.[29] The PU used in this study can be categorized as a TPU with a hardness of 80 on the shore A scale. The soft segmented PUs exhibited a mechanical strain of approximately 550% and 570% with rapidly increasing mechanical stress of 32 MPa and 15 MPa, respectively.[30]

3.2. Gas Permeation Measurement. The gas barrier properties of the TPU and TPU-based films (TPU/Au and GBF) were investigated using oxygen, and the results are shown in Figure 3. The thickness of the films varied between 200 and 330 μm. The oxygen transmission rates (OTRs) of the films were measured using a gas chromatograph. The stretchable GBF showed an excellent barrier performance of 0 cc/m^2/24 h/atm OTR in both nonstretched and stretched conditions. The OTR of Al-laminated film, usually used as a packaging material for pouch cell batteries, is shown in Figure 3A. The same quantity of gas permeation (0 cc/m^2/24 h/atm) was measured in the Al-laminated film. In the nonstretched condition, the TPU/Au film exhibited a better result of 774 cc/m^2/24 h/atm, which was smaller by a factor of approximately 84%, when compared to the TPU film (4998 cc/m^2/24 h/atm). In the stretched condition, the gas permeation in the TPU/Au film was approximately 51% lesser (2661 cc/m^2/24 h/atm) than in the TPU film (5513 cc/m^2/24 h/atm), as shown in Figure 3A,B. Moreover, the OTR values of the TPU, TPU/Au, and GBF were measured after stretch−release cycles of 1, 10, 50, 100, 150, and 200, as shown in Figure 3C. At the mechanical strain of 50%, the TPU/Au film presented a lower gas permeation than the TPU film for all stretch−release cycles. As the number of stretch−release cycles increased, the gas permeation through the films increased owing to the plasticity of the TPU film. However, there were cases where the gas permeation decreased over the stretch−release cycles as the gas permeation area of the films differed. Furthermore, the gas permeation rates of the TPU film, TPU/Au film, and GBF were compared to those of PDMS and Ecoflex-0030 films by measuring gas permeation rates of PDMS and Ecoflex-0030 films on stretch−release cycles. The outcomes of these measurements are illustrated in Figure S6. The thicknesses of the PDMS and Ecoflex-0030 films coated with Au and LM layers were between 200 and 420 μm, respectively. The Ecoflex-0030/Au/LM/Ecoflex-0030 film showed a higher OTR than the PDMS/Au/LM/PDMS film. Notably, the gas permeation was significantly reduced when the LM was coated on the substrate films. Additionally, the gas permeation rate measurement was also conducted using nitrogen gas on the TPU film, TPU/Au film, and the GBF for nonstretched and stretched states and after stretch−release cycles, shown in Figure S7. The GBF exhibited similar results for the three states as those obtained using oxygen, which was

https://doi.org/10.1021/acsami.2c13023
ACS Appl. Mater. Interfaces XXXX, XXX, XXX−XXX

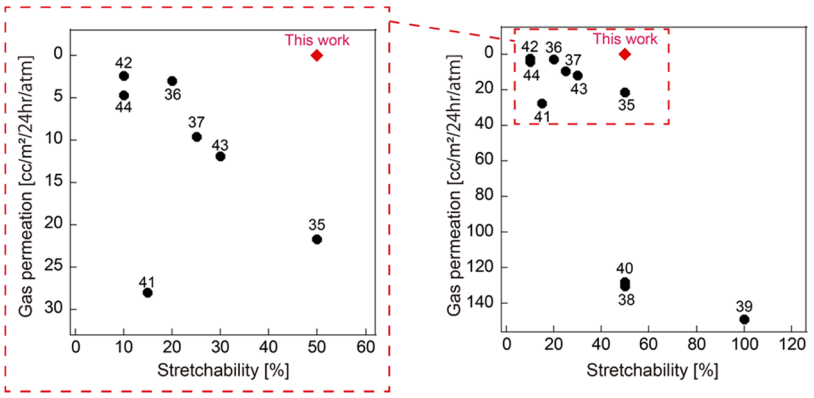

Figure 4. Comparison of gas permeation and stretchability in other stretchable GBFs with that in the proposed stretchable GBF. The proposed stretchable GBF shows a higher gas impermeability with good stretchability than that in other stretchable GBFs.

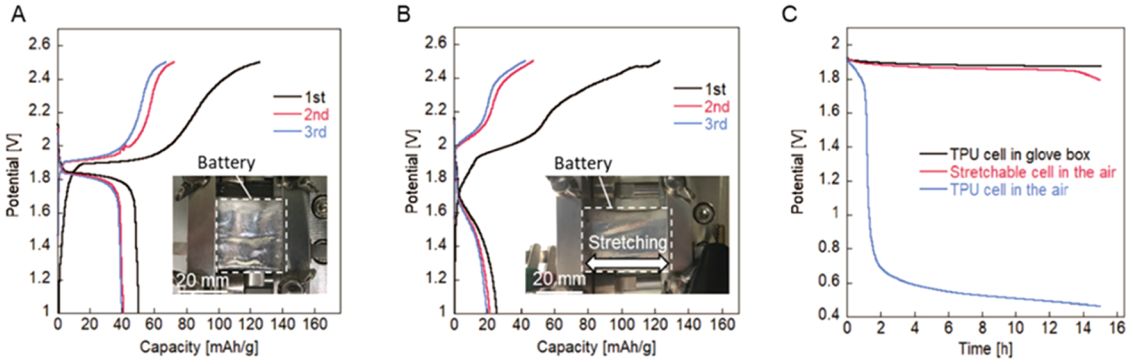

Figure 5. Characteristics of a highly deformable battery. Charge−discharge curve specifying the specific capacity in (A) the original state and (B) 50% stretched state. (C) Decrease in potential over time under ambient conditions.

"0 cc/m^2/24 h/atm". Thus, the measured OTR values of the stretchable GBF indicate excellent performance.

Moisture permeation of the GBF, Al-laminated film, which is specially made for Li-ion batteries, TPU film, PDMS, and Ecoflex-0030 films was measured. The Al-laminated film had the lowest moisture permeation of approximately zero, followed by the GBF. Unlike the Al-laminated film, the GBF could not prevent moisture permeation completely though it was significantly suppressed when compared with moisture permeation of the TPU, PDMS, and Ecoflex-0030 films. Determining the high moisture impermeability of stretchable GBF is difficult, even though its capability to resist moisture was proven because moisture permeation in the stretchable GBF slightly increased over time. Moreover, moisture permeation measurement was conducted on the stretchable GBF with different LM thicknesses of 4.5, 11.23, 19.4, and 31.7 μm, as shown in Figure S13. The moisture permeation can be sufficiently prevented with an LM thickness of 11.23 μm or more. However, the LM with a thickness of approximately 20 μm becomes unstable and may lead to leakage, which can be disruptive to the fabrication of the highly deformable battery. The moisture permeation of the GBF may have been affected by a change in the oxide layer formed on the outer surface of the LM owing to air exposure. Studies show that when water meets the LM, it breaks the Ga_2O_3 oxide layer formed by air exposure and a new oxide layer of GaOOH with a fresh LM is again formed.[31−34] During the moisture permeation measurement, there was an excess of water above the normal atmosphere. Thus, excess water may have decreased the yielded stress and storage modulus of the oxide layer and also weakened the LM.

In Figure 4, stretchable GBFs from other studies are compared with that proposed in this study. A layer-by-layer method was used to fabricate these stretchable GBFs. According to the existing literature,[35−44] gas permeation can be reduced by increasing the number of layers. Mostly, polyethylene oxide, polyacrylic acid, graphene oxide (GO), polyethylenimine, and montmorillonite clay platelets were utilized to build the GBF layers, which varied up to 60 layers. Stretchable GBFs based on the PU rubber substrate are also available, where 10−30 multilayers are deposited on a 1 mm thick PU rubber film. Compared to the PU substrate film, the gas permeation was reduced by 46, 7, and 15 times at strains of 20, 25, and 50%, respectively.[35−37] Similarly, 40 bilayers deposited on a 1.6 mm thick natural rubber substrate aided the reduction by up to 29 times, at an average strain of 100%, when compared to a bare substrate film.[38−40] The multilayered film using PU and GO platelets exhibited an 80% reduction of gas permeation when compared to that in polyethylene-terephthalate substrate film.[41] Thus, clay platelets reduce gas permeation. The clay platelet films with 30 multilayers managed to reduce gas permeation by 15 times when compared to that by the bare PDMS/Ecoflex substrate film.[42,43] Moreover, thinner GBF with a thickness of 35 nm, based on polyamide 2,3 and hafnium oxide (HfO2), was fabricated by atomic and molecular layer deposition. It presented a 4.2 cc/m^2/24 h He-gas permeation rate at a strain of 10%.[44]

https://doi.org/10.1021/acsami.2c13023
ACS Appl. Mater. Interfaces XXXX, XXX, XXX−XXX

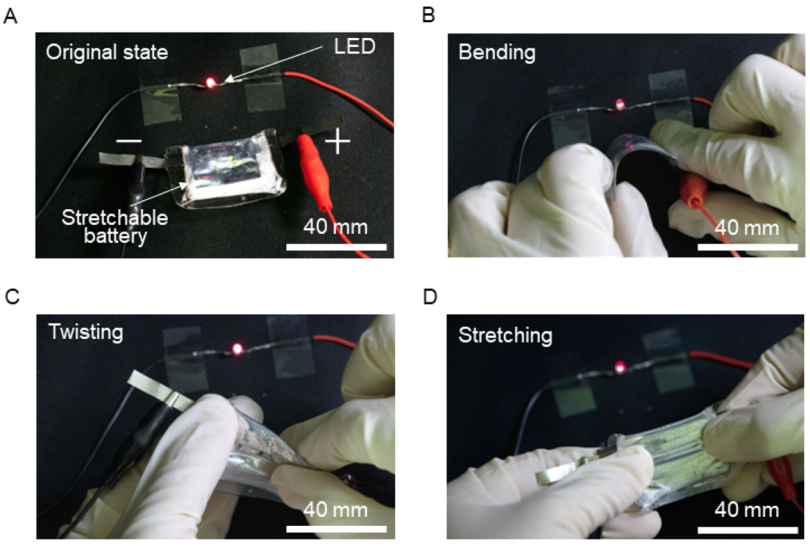

Figure 6. Demonstration of a highly deformable battery powering LED in air when in the (A) original state (no deformation) and under mechanical deformations, such as (B) 90° bending, (C) approximately 25° twisting, and (D) stretching by a 50% strain.

The gas permeation reduction rate is affected not only by the number of layers but also by the materials and fabrication methods adopted. As shown in Figure 4, when stretchability increases, gas permeation increases. The stretchability of the GBF was limited to 10% for lower gas permeations. However, the proposed stretchable GBF was able to prevent gas permeation completely at a strain of 50%. Thus, stretchability can be increased by over 50%.

3.3. Characteristics of the Highly Deformable Battery. The proposed GBF was demonstrated by fabricating a highly deformable battery based on stretchable LTO/LFP electrodes. As the TPU film was used to completely seal the LM, no LM leakage from the GBF was observed that could induce a short circuit of the highly deformable battery. Figure 5A,B illustrates the electrochemical characteristics of the highly deformable battery by conducting a charge−discharge measurement. The fabricated highly deformable battery maintained a potential of 1.8 V, with and without deformation. It delivered a capacity of approximately 50 and 25 mAh/g in the original state and 50% stretched state, respectively. When the battery was stretched throughout the measurement, its capacity decreased by 50%. The capacity and cycle performance of the battery were lower than the theoretical value and result in other reported LTO/LFP batteries,[45] possibly due to the high internal resistance and low utilization of active materials in the SBS-based stretchable electrodes. An electrochemical measurement was conducted on the half-cells based on LFP- and LTO-stretchable electrodes, and their capacity was measured as approximately 145 and 160 mAh/g, respectively. On average, the Coulombic efficiencies of the LFP and LTO electrodes were 90 and 100%, respectively, as shown in Figure S10. The lower Coulombic efficiency of the LFP electrode was probably due to the oxidative decomposition of the unsaturated C═C groups of polybutadiene-blocks in the SBS. Thus, the Coulombic efficiency of the battery as a full cell was low at the beginning, and from the 4th cycle onwards, it stabilized at 80%, as shown in Figure S11B.[46,47] The reported stretchable or flexible batteries differed in their outer shapes or designs, such as wavy, foldable, and fiberlike, selection of active materials, and stretchability. However, their capacities were stable even under strain. The capacity of the deformable batteries dropped to approximately 20%, from the initial capacity, when a mechanical stress was applied.[48−56] Thus, stretchability was limited by battery designs. The accordion-like,[48] kirigami,[49] arched structure,[50] origami,[51] and wire-shaped[52] stretchable lithium-ion batteries presented a stable capacity of approximately 130−150 mAh/g under stretchability in the range of 8−400%. The battery, using LTO/LFP as active materials with a simple design, delivered a capacity of approximately 130 mAh/g under an 80% strain and up to 500 stretch−release cycles.[53] Similarly, a stretchable battery, using the same active materials, delivered a capacity of 120 mAh/g and approximately 118 mAh/g before and after 50% strain, respectively. The battery capacity was reduced by 1.6% after stretching.[45] Other than the outer design of the stretchable battery, its inner components must be flexible and should maintain a stable operation. The process of lithium (Li) plating and stripping in a battery is essential for its stability. For stable Li plating and stripping, polymer electrolytes based on the TPU and anode electrodes based on lithium polyacrylic acid were developed, which satisfied both stable cycling performance and good flexibility. A stable operation can also be ensured by adding a protective and water-proof layer on the Li metal anode surface to avoid dendrite growth and corrosion.[57−59]

The SBS-based stretchable electrodes can be further optimized for practical use. However, for this study, the performance of the fabricated highly deformable battery was sufficient for analyzing the properties of the stretchable GBF. A galvanostatic discharge experiment was performed in air. Figure 5C illustrates the outcome of the galvanostatic discharge experiment conducted on the fabricated highly deformable batteries packaged using the GBF and a bare TPU film. Evidently, the fabricated battery packaged using the bare TPU film only (TPU cell) worked inside an argon gas-filled glovebox and not in air. A constant potential was maintained throughout when operated inside the argon gas-filled glovebox. By maintaining a constant potential for over 14 h, the fabricated highly deformable battery packaged using the GBF demonstrated a better operation in air than that of the battery packaged using the bare TPU film. However, the potential gradually dropped after 16 h, possibly due to moisture permeation through the GBF, as GBF cannot be protected

https://doi.org/10.1021/acsami.2c13023
ACS Appl. Mater. Interfaces XXXX, XXX, XXX−XXX

from the moisture completely, as shown in Figure 3D. These results indicate that the GBF requires further improvement for its long-term use in air. Nevertheless, the proposed LM-coated GBF can serve as a packaging material solution to overcome the current limitations in deformable batteries.

Additionally, a red light-emitting diode (LED) was powered by the fabricated highly deformable battery in air under mechanical deformations, including bending, twisting, and stretching, as shown in Figure 6. The highly deformable battery maintained a constant potential of 1.8 V, while the LED was successfully lighted during the bending (Video S1), twisting (Video S2), and stretching (Video S3) states by approximately 90°, 25°, and 50% strain, respectively. Thus, the fabricated highly deformable battery is capable of powering actual devices that require stretchability or flexibility.

4. CONCLUSIONS

In this study, a stretchable LM-based packaging film with excellent gas and moisture impermeability is developed using a simple layer-by-layer method. The gas permeation of the stretchable packaging film (GBF) was measured to be 0 cc/m^2/24 h/atm, while moisture permeation was approximately zero. The highly deformable battery, fabricated using the proposed packaging film, presents excellent operational stability in air even for small durations, although its capacity is not favorable because of the battery functionality. Owing to its low moisture permeation, the stretchable GBF is not suited for the reliable storage of highly deformable batteries. The stretchable GBF can be further improved to enhance its moisture protection ability by modifying the constituent materials. In addition, further improvements to stabilize the performance of the highly deformable battery, even under deformation, can be done by developing materials for its constituent parts. However, the findings of this study indicate the potential usage of highly deformable batteries, which have a high energy density, high working voltage, and long-term stability, in realizing good stretchable and flexible devices, without using the bulky batteries that are currently trending. The proposed stretchable packaging film is more beneficial than the Al-laminated film, which is often used in bulk batteries, for wearable electronic devices because of its flexibility and easy deformability. This work is among the first few studies conducted on a combination of a highly deformable battery, which can be used in the air, and stretchable packaging film.

■ ASSOCIATED CONTENT

Supporting Information

The Supporting Information is available free of charge at https://pubs.acs.org/doi/10.1021/acsami.2c13023.

Wettability of LM on TPU, cross-sectional SEM−EDX, gas permeation analysis on PDMS- and Ecoflex-0030-based films, additional gas permeation analysis on TPU-based films with nitrogen gas, and electrochemical measurement of coin cell using stretchable electrodes (PDF)

Demonstration of the highly deformable battery under mechanical deformations in air during bending (Video S1) (MP4)

Demonstration of the highly deformable battery under mechanical deformations in air during twisting (Video S2) (MP4)

Demonstration of the highly deformable battery under mechanical deformations in air during stretching (Video S3) (MP4)

■ AUTHOR INFORMATION

Corresponding Author

Hiroki Ota − *Department of Mechanical Engineering, Yokohama National University, Yokohama 240-8501, Japan;* orcid.org/0000-0002-3702-6357; Email: ota-hiroki-xm@ynu.ac.jp

Authors

Nyamjargal Ochirkhuyag − *Department of Mechanical Engineering, Yokohama National University, Yokohama 240-8501, Japan;* orcid.org/0000-0001-8526-3990

Yuuki Nishitai − *Department of Mechanical Engineering, Yokohama National University, Yokohama 240-8501, Japan*

Satoru Mizuguchi − *Department of Mechanical Engineering, Yokohama National University, Yokohama 240-8501, Japan*

Yuji Isano − *Department of Mechanical Engineering, Yokohama National University, Yokohama 240-8501, Japan*

Sijie Ni − *Department of Mechanical Engineering, Yokohama National University, Yokohama 240-8501, Japan*

Koki Murakami − *Department of Mechanical Engineering, Yokohama National University, Yokohama 240-8501, Japan*

Masaki Shimamura − *Department of Mechanical Engineering, Yokohama National University, Yokohama 240-8501, Japan*

Hiroki Iida − *Department of Chemistry and Life Science, Yokohama National University, Yokohama 240-8501, Japan*

Kazuhide Ueno − *Department of Chemistry and Life Science, Yokohama National University, Yokohama 240-8501, Japan;* orcid.org/0000-0002-4684-5717

Complete contact information is available at: https://pubs.acs.org/10.1021/acsami.2c13023

Author Contributions

N.O. and Y.N. collected data and conducted experiments for this study. S.M. carried out fundamental experiments. Y.I. helped to collect data on moisture permeation measurement. S.N. helped to collect data from the SEM−EDX analysis. K.M. helped to measure the LM layer thickness. M.S. helped to collect data on repeatability measurement. H.I. helped to collect data on gas permeation measurement. K.U. reviewed and guided the progress of paper writing. H.O. supervised and guided the research. N.O. and H.O. wrote the paper.

Notes

The authors declare no competing financial interest.

■ ACKNOWLEDGMENTS

This research was supported partly by JSPS KAKENHI (Grant No. 20H00213), Pfizer Health Research Foundation, and JST CREST (Grant Number JPMJCR1905), Japan.

■ ABBREVIATIONS USED

LM, liquid metal
GBF, gas barrier film
TPU, thermoplastic polyurethane
PDMS, polydimethylsiloxane
SBS, polystyrene-*block*-polybutadiene-*block*-polystyrene
LTO, lithium titanium oxide
LFP, lithium iron phosphate

REFERENCES

(1) Song, W.-J.; Yoo, S.; Song, G.; Lee, S.; Kong, M.; Rim, J.; Jeong, U.; Park, S. Recent Progress in Stretchable Batteries for Wearable Electronics. *Batteries Supercaps* **2019**, *2*, 181−199.

(2) Zhai, Q.; Xiang, F.; Cheng, F.; Sun, Y.; Yang, X.; Lu, W.; Dai, L. Recent Advances in Flexible/Stretchable Batteries and Integrated Devices. *Energy Storage Mater.* **2020**, *33*, 116−138.

(3) Choi, S.; Lee, H.; Ghaffari, R.; Hyeon, T.; Kim, D. H. Recent Advances in Flexible and Stretchable Bio-Electronic Devices Integrated with Nanomaterials. *Adv. Mater.* **2016**, *28*, 4203−4218.

(4) Fan, X.; Liu, B.; Ding, J.; Deng, Y.; Han, X.; Hu, W.; Zhong, C. Flexible and Wearable Power Sources for Next-Generation Wearable Electronics. *Batteries Supercaps* **2020**, *3*, 1262−1274.

(5) Shi, Q.; Dong, B.; He, T.; Sun, Z.; Zhu, J.; Zhang, Z.; Lee, Ch. Progress in Wearable Electronics/Photonics—Moving Toward the Era of Artificial Intelligence and Internet of Things. *InfoMat.* **2020**, *2*, 1131−1162.

(6) Chen, D.; Lou, Z.; Jiang, K.; Shen, G. Device Configurations and Future Prospects of Flexible/Stretchable Lithium-Ion Batteries. *Adv. Funct. Mater.* **2018**, *28*, No. 1805596.

(7) Wehner, L. A.; Mittal, N.; Liu, T.; Niederberger, M. Multifunctional Batteries: Flexible, Transient, and Transparent. *ACS Cent. Sci.* **2021**, *7*, 231−244.

(8) Hong, S. Y.; Jee, S. M.; Ko, Y.; Cho, J.; Lee, K. H.; Yeom, B.; Kim, H.; Son, J. G. Intrinsically Stretchable and Printable Lithium-Ion Battery for Free-Form Configuration. *ACS Nano.* **2022**, *16*, 2271−2281.

(9) Song, W. J.; Lee, S.; Song, G.; Park, S. Stretchable Aqueous Batteries: Progress and Prospects. *ACS Energy Lett.* **2019**, *4*, 177−186.

(10) Mackanic, D. G.; Chang, T. H.; Huang, Z.; Cui, Y.; Bao, Z. Stretchable Electrochemical Energy Storage Devices. *Chem. Soc. Rev.* **2020**, *49*, 4466−4495.

(11) Shin, M.; Song, W. J.; Son, H. B.; Yoo, S.; Kim, S.; Song, G.; Choi, N. S.; Park, S. Highly Stretchable Separator Membrane for Deformable Energy-Storage Devices. *Adv. Energy Mater.* **2018**, *8*, No. 1801025.

(12) Ock, J.-Y.; Fujishiro, M.; Ueno, K.; Watanabe, M.; Dokko, K. Electrochemical Properties of Poly (vinylidene fluoride-co-hexafluoropropylene) Gel Electrolytes with High-Concentration Li Salt/Sulfolane for Lithium Batteries. *Electrochemistry* **2021**, *89*, 567−572.

(13) Handschuh-Wang, S.; Zhu, L.; Wang, T. Is There a Relationship between Surface Wettability of Structured Surfaces and Lyophobicity toward Liquid Metals? *Materials* **2020**, *13*, 2283.

(14) Yousefi, E.; Sun, Y.; Kunwar, A.; Guo, M.; Moelans, N.; Seveno, D. Surface Tension of Aluminum-Oxygen system: A molecular Dynamics Study. *Acta Mater.* **2021**, *221*, No. 117430.

(15) Zhao, X.; Xu, S.; Liu, J. Surface tension of Liquid Metal: Role, Mechanism and Application. *Front. Energy Res.* **2017**, *11*, 535−567.

(16) Johansson, P.; Lahti, J.; Vihinen, J.; Kuusipalo, J. Permeability of Oxygen and Carbon Dioxide Through Pinholes in Barrier Coatings. *J. Appl. Packag. Res.* **2019**, *11*, 49−63.

(17) Li, G.; Wu, X.; Lee, D-W. Selectively Plated Stretchable Liquid Metal Wires for Transparent Electronics. *Sens. Actuators B Chem.* **2015**, *221*, 1114−1119.

(18) Park, S.; Thangavel, G.; Parida, K.; Li, S.; Lee, P. S. A Stretchable and Self-Healing Energy Storage Device Based on Mechanically and Electrically Restorative Liquid-Metal Particles and Carboxylated Polyurethane Composites. *Adv. Mater.* **2019**, *31*, No. 1805536.

(19) Tutika, R.; Haque, A. B. M. T.; Bartlett, M. D. Self-healing Liquid Metal Composite for Reconfigurable and Recyclable Soft Electronics. *Commun. Mater.* **2021**, *2*, 64.

(20) Zhu, H.; Wang, S.; Zhang, M.; Li, T.; Hu, G.; Kong, D. Fully Solution Processed Liquid Metal Features as Highly Conductive and Ultrastretchable Conductors. *npj Flex Electron.* **2021**, *5*, 25.

(21) Bhuyan, P.; Wei, Y.; Sin, D.; Yu, J.; Nah, C.; Jeong, K. U.; Dickey, M. D.; Park, S. Soft and Stretchable Liquid Metal Composites with Shape Memory and Healable Conductivity. *ACS Appl. Mater. Interfaces* **2021**, *13*, 28916−28924.

(22) Bartlett, M. D.; Fassler, A.; Kazem, N.; Markvicka, E. J.; Mandal, P.; Majidi, C. Stretchable, High-k Dielectric Elastomers through Liquid-Metal Inclusions. *Adv. Mater.* **2016**, *28*, 3726−3731.

(23) Wu, N.; Cao, Q.; Wang, X.; Li, X.; Deng, H. A Novel High-Performance Gel Polymer Electrolyte Membrane Basing on Electrospinning Technique for Lithium Rechargeable Batteries. *J. Power Sources* **2011**, *196*, 8638−8643.

(24) Wu, N.; Cao, Q.; Wang, X.; Li, S.; Li, X.; Deng, H. In situ Ceramic Fillers of Electrospun Thermoplastic Polyurethane/poly-(vinylidene fluoride) Based Gel Polymer Electrolytes for Li-ion Batteries. *J. Power Sources* **2011**, *196*, 9751−9756.

(25) Petrović, Z. S.; Ferguson, J. Polyurethane Elastomers. *Prog. Polym. Sci.* **1991**, *16*, 695−836.

(26) Hu, J.; Yang, R.; Zhang, L.; Chen, Y.; Sheng, X.; Zhang, X. Robust, Transparent, and Self-Healable Polyurethane Elastomer via Dynamic Crosslinking of Phenol-Carbamate Bonds. *Polymer* **2021**, *222*, No. 123674.

(27) Madbouly, S. A. Waterborne Polyurethane Dispersions and Thin Films: Biodegradation and Antimicrobial Behaviors. *Molecules* **2021**, *26*, 961.

(28) Prisacariu, C.; Scortanu, E.; Stoica, I.; Agapie, B.; Barboiu, V. Morphological Features and Thermal and Mechanical Response in Segmented Polyurethane Elastomers Based on Mixtures of Isocyanates. *Polym. J.* **2011**, *43*, 613−620.

(29) Reis, J. M. L.; Chaves, F. L.; da Costa Mattos, H. S. Tensile Behaviour of Glass Fibre Reinforced Polyurethane at Different Strain Rates. *Mater. Des.* **2013**, *49*, 192−196.

(30) Christenson, E. M.; Anderson, J. M.; Hiltner, A.; Baer, E. Relationship between Nanoscale Deformation Processes and Elastic Behavior of Polyurethane Elastomers. *Polymer* **2005**, *46*, 11744−11754.

(31) Khan, M. R.; Trlica, C.; So, J. H.; Valeri, M.; Dickey, M. D. Influence of Water on the Interfacial Behavior of Gallium Liquid Metal Alloys. *ACS Appl. Mater. Interfaces* **2014**, *6*, 22467−22473.

(32) Jacob, A. R.; Parekh, D. P.; Dickey, M. D.; Hsiao, L. C. Interfacial Rheology of Gallium-Based Liquid Metals. *Langmuir* **2019**, *35*, 11774−11783.

(33) Creighton, M. A.; Yuen, M. C.; Susner, M. A.; Farrell, Z.; Maruyama, B.; Tabor, C. E. Oxidation of Gallium-based Liquid Metal Alloys by Water. *Langmuir* **2020**, *36*, 12933−12941.

(34) Tang, S-Y.; Qiao, R. Liquid Metal Particles and Polymers: A Soft−Soft System with Exciting Properties. *Acc. Mater. Res.* **2021**, *2*, 966−978.

(35) Cho, C.; Xiang, F.; Wallace, K. L.; Grunlan, J. C. Combined Ionic and Hydrogen Bonding in Polymer Multilayer Thin Film for High Gas Barrier and Stretchiness. *Macromolecules* **2015**, *48*, 5723−5729.

(36) Qin, S.; Song, Y.; Floto, M. E.; Grunlan, J. C. Combined High Stretchability and Gas Barrier in Hydrogen-Bonded Multilayer Nanobrick Wall Thin Films. *ACS Appl. Mater. Interfaces* **2017**, *9*, 7903−7907.

(37) Cho, C.; Song, Y.; Allen, R.; Wallace, K. L.; Grunlan, J. C. Stretchable Electrically Conductive and High Gas Barrier Nanocomposites. *J. Mater. Chem. C* **2018**, *6*, 2095−2104.

(38) Xiang, F.; Ward, S. M.; Givens, T. M.; Grunlan, J. C. Super Stretchy Polymer Multilayer Thin Film with High Gas Barrier. *ACS Macro Lett.* **2014**, *3*, 1055−1058.

(39) Xiang, F.; Givens, T. M.; Ward, S. M.; Grunlan, J. C. Elastomeric Polymer Multilayer Thin Film with Sustainable Gas Barrier at High Strain. *ACS Appl. Mater. Interfaces* **2015**, *7*, 16148−16151.

(40) Shi, K.; Xu, X.; Dong, S.; Li, B.; Han, J. Stretchable Gas Barrier Films Achieved by Hydrogen-Bond Self-Assembly of Nano-Brick Multilayers. *AIChE J.* **2021**, *67*, No. e17373.

(41) Noh, M. J.; Oh, M. J.; Choi, J. H.; Yu, J. C.; Kim, W. J.; Park, J.; Chang, Y. W.; Yoo, P. J. Layer-by-layer Assembled Multilayers of Charged Polyurethane and Graphene Oxide Platelets for Flexible and Stretchable Gas Barrier Films. *Soft Matter.* **2018**, *14*, 6708−6715.

https://doi.org/10.1021/acsami.2c13023
ACS Appl. Mater. Interfaces XXXX, XXX, XXX−XXX

(42) Holder, K. M.; Spears, B. R.; Huff, M. E.; Priolo, M. A.; Harth, E.; Grunlan, J. C. Stretchable Gas Barrier Achieved with Partially Hydrogen-Bonded Multilayer Nanocoating. *Macromol. Rapid Commun.* **2014**, *35*, 960−964.
(43) Kim, S.; Kim, T.; Kim, D.; Ju, B. K. Layer-by-Layer Assembled Nano-Composite Multilayer Gas Barrier Film Manufactured with Stretchable Substrate. *Appl. Sci.* **2021**, *11*, 5794.
(44) Tseng, M. H.; Su, D.-Y.; Chen, G. L.; Tsai, F. Y. Nano-Laminated Metal Oxides/Polyamide Stretchable Moisture- and Gas-Barrier Films by Integrated Atomic/Molecular Layer Deposition. *ACS Appl. Mater. Interfaces* **2021**, *13*, 27392−27399.
(45) Tian, M.; Qi, Y.; Oh, E.-S. Application of a Polyacrylate Latex to a Lithium Iron Phosphate Cathode as a Binder Material. *Energies* **2021**, *14*, 1902.
(46) Yabuuchi, N.; Kinoshita, Y.; Misaki, K.; Matsuyama, T.; Komaba, S. Electrochemical Properties of LiCoO2 Electrodes with Latex Binders on High-Voltage Exposure. *J. Electrochem. Soc.* **2015**, *162*, A538.
(47) Shi, C.; Wang, T.; Liao, X.; Qie, B.; Yang, P.; Chen, M.; Wang, X.; Srinivasan, A.; Cheng, Q.; Ye, Q.; Li, A. C.; Chen, X.; Yang, Y. Accordion-like stretchable Li-ion batteries with High Energy Density. *Energy Storage Mater.* **2019**, *17*, 136−142.
(48) Song, Z.; Wang, X.; Lv, C.; An, Y.; Liang, M.; Ma, T.; He, D.; Zheng, Y. J.; Huang, S. Q.; Yu, H.; Jiang, H. Kirigami-based Stretchable Lithium-ion Batteries. *Sci Rep.* **2015**, *5*, No. 10988.
(49) Weng, W.; Sun, Q.; Zhang, Y.; He, S.; Wu, Q.; Deng, J.; Fang, X.; Guan, G.; Ren, J.; Peng, H. A Gum-Like Lithium-Ion Battery Based on a Novel Arched Structure. *Adv. Mater.* **2015**, *27*, 1363−1369.
(50) Song, Z.; Ma, T.; Tang, R.; Cheng, Q.; Wang, X.; Krishnaraju, D.; Panat, R.; Chan, C. K.; Yu, H.; Jiang, H. Origami Lithium-ion Batteries. *Nat. Commun.* **2014**, *5*, No. 3140.
(51) Hoshide, T.; Zheng, Y.; Hou, J.; Wang, Z.; Li, Q.; Zhao, Z.; Ma, R.; Sasaki, T.; Geng, F. Flexible Lithium-Ion Fiber Battery by the Regular Stacking of Two-Dimensional Titanium Oxide Nanosheets Hybridized with Reduced Graphene Oxide. *Nano Lett.* **2017**, *17*, 3543−3549.
(52) Liu, W.; Chen, Z.; Zhou, G.; Sun, Y.; Lee, H. R.; Liu, C.; Yao, H.; Bao, Z.; Cui, Y. 3D Porous Sponge-Inspired Electrode for Stretchable Lithium-Ion Batteries. *Adv. Mater.* **2016**, *28*, 3578−3583.
(53) Kang, S.; Hong, S. Y.; Kim, N.; Oh, J.; Park, M.; Chung, K. Y.; Lee, S. S.; Lee, J.; Son, J. G. Stretchable Lithium-Ion Battery Based on Re-entrant Micro-honeycomb Electrodes and Cross-Linked Gel Electrolyte. *ACS Nano* **2020**, *14*, 3660−3668.
(54) Wang, X.; Lu, Y.; Geng, D.; Li, L.; Zhou, D.; Ye, H.; Zhu, Y.; Wang, R. Planar Fully Stretchable Lithium-Ion Batteries Based on a Lamellar Conductive Elastomer. *ACS Appl. Mater. Interfaces* **2020**, *12*, 53774−53780.
(55) Liu, K.; Kong, B.; Liu, W.; Sun, Y.; Song, M. S.; Chen, J.; Liu, Y.; Lin, D.; Pei, A.; Cui, Y. Stretchable Lithium Metal Anode with Improved Mechanical and Electrochemical Cycling Stability. *Joule* **2018**, *2*, 1857−1865.
(56) Gu, T.; Cao, Z.; Wei, B. All-Manganese-Based Binder-Free Stretchable Lithium-Ion Batteries. *Adv. Energy Mater.* **2017**, *7*, No. 1700369.
(57) Li, N.-W.; Shi, Y.; Yin, Y.-X.; Zeng, X.-X.; Li, J.-Y.; Li, C.-J.; Wan, L.-J.; Wen, R.; Guo, Y.-G. A Flexible Solid Electrolyte Interphase Layer for Long-Life Lithium Metal Anodes. *Angew. Chem. Int. Ed.* **2018**, *57*, 1505−1509.
(58) Wu, N.; Shi, Y-R.; Lang, S-Y.; Zhou, J-M.; Liang, J-Y.; Wang, W.; Tan, S-J.; Yin, Y-X.; Wen, R.; Guo, Y-G. Self-Healable Solid Polymeric Electrolytes for Stable and Flexible Lithium Metal Batteries. *Angew. Chem.* **2019**, *131*, 18314−18317.
(59) Zhou, L.; Zhao, M.; Chen, X.; Zhou, J.; Wu, M.; Wu, N. A Hydrophobic Artificial Solid-Interphase-Protective Layer with Fast Self-Healable Capability for Stable Lithium Metal Anodes. *Sci. China Chem.* **2022**, *65*, 1817.

https://doi.org/10.1021/acsami.2c13023
ACS Appl. Mater. Interfaces XXXX, XXX, XXX−XXX